

Miocene to Messinian deformation and hydrothermal activity in a pre-Alpine basement massif of the French western Alps: new U-Th-Pb and argon ages from the Lauzière massif

DOMINIQUE GASQUET¹, JEAN-MICHEL BERTRAND², JEAN-LOUIS PAQUETTE³, JÉRÉMIE LEHMANN⁴, GUEORGUI RATZOV⁵, ROGER DE ASCENÇÃO GUEDES⁶, MASSIMO TIEPOLO⁷, ANNE-MARIE BOULLIER⁸, STÉPHANE SCAILLET⁹ and SÉBASTIEN NOMADE⁹

Key-words. – Hydrothermal veins, U-Pb and Ar-Ar geochronology, Miocene, Lauzière, External crystalline, Western Alps

Abstract. – U-Pb and Th-Pb dating of monazite from hydrothermal quartz veins (“Alpine veins”) from the Lauzière massif (North Belledonne) together with Ar/Ar ages of adularias from the same veins constrain the age of the last tectono-metamorphic events that affected the External Crystalline Massifs (ECM). Ages obtained are surprisingly young. The study of the structural context of the veins combined with our chronological data, allow us to propose a tectonic scenario of the northern ECM for the 15-5 Ma period, which was poorly documented so far.

The quartz veins are of two types: (i) the oldest are poorly mineralized (chlorite and epidote), flat-lying veins. The quartz fibres (= extension direction) are near vertical and seem to be associated with a subvertical dissolution schistosity superimposed upon an early Alpine deformation underlined by “mini-biotite”. They bear a sub-horizontal stretching lineation; (ii) the youngest veins are very rich in various minerals (anatase, rutile, phénacite, meneghinite, beryl, synchysite,). They are almost vertical. Their “en echelon” geometry as well as the horizontal attitude of their quartz fibres show a dextral strike-slip regime. Two groups of Th-Pb ages have been obtained: 11 to 10 Ma and 7 to 5 Ma. They were obtained from the most recent veins (vertical veins) sampled in different areas of the massif. The ca. 10 Ma ages are related to veins in the Lauzière granite and its metamorphic country-rocks at about 2 km from the eastern contact of the massif, while the ages of ca. 5 Ma correspond to veins occurring in mylonites along this contact. Adularias provided Ar/Ar ages at ca. 7 Ma. By contrast, a monazite from a vein of the Pelvoux massif (Plan du Lac) yielded a Th-Pb age of 17.6 Ma but in a different structural setting. Except fission track ages, there are very little ages of this range published in the recent literature on the Alps. The latter concern always gold mineralized veins (NE Mont Blanc and SW Lepontine dome). The last compressive tectonic regime dated between 15 and 12 Ma is coeval with (i) the late “Roselend thrust” event, which is recorded in the Mont Blanc by shear-zones with vertical lineation, (ii) the last movements in the basal mylonites of the Swiss Nappes, (iii) the horizontal Alpine veins from the Mont Blanc and Belledonne massifs (with vertical quartz fibres), which are similar to the early veins of the Lauzière. On the contrary, the vertical veins of the Lauzière, dated between 11 and 5 Ma, correspond to a dextral strike slip regime. This suggests that most of the strike-slip tectonics along the ECM took place during two stages (ca. 10 Ma and ca. 7-5 Ma) and not only at 18 Ma as had been proposed previously. Our ages are consistent with the late Miocene-Pliocene overlap of the Digne thrust to the South and to part of the normal movement along the Simplon fault to the North. Thus, all the external crystalline massifs were tectonically active during the late Miocene. This suggests that tectonic events in the external alpine belt may have contributed to some extent to the geodynamical causes of the Messinian crisis.

Déformation et hydrothermalisme Miocène à Messinien dans le massif de la Lauzière (Alpes occidentales françaises) : nouveaux âges U-Th-Pb et argon

Mots-clés. – Veines hydrothermales, Géochronologie U-Pb and Ar-Ar, Miocène, Lauzière, Massifs cristallins externes, Alpes occidentales.

Résumé. – Des datations U-Pb, Th-Pb de monazite hydrothermale dans des veines de quartz (fentes alpines) du massif de la Lauzière, au nord de Belledonne et Ar/Ar sur des adulaires des mêmes veines ont permis de préciser l'âge des derniers événements tectono-métamorphiques alpins dans les massifs cristallins externes (MCE) des Alpes. Les résultats obtenus sont surprenants car très jeunes, et l'étude du contexte structural des veines a permis, combinés aux âges, de proposer un scénario tectonique pour le « Cristallin Externe » du Nord pour la période 15-5 Ma, très mal documentée jusqu'à présent.

1. EDYTEM, Université de Savoie, CISM-EDYTEM, CNRS – UMR 5204, Domaine Scientifique, 73376 Le Bourget du Lac cedex, France, Tel: 33 (0)4 79 75 86 45, Fax: 33 (0)4 79 75 87 77, dominique.gasquet@univ-savoie.fr

2. LGCA, CNRS, Université de Savoie, France

3. CNRS, Université Blaise Pascal, Clermont-Ferrand, France

4. CGS-EOST, CNRS, Université de Strasbourg, France

5. Géosciences Azur, CNRS, Université de Nice-Sophia Antipolis, France

6. Le Règne Minéral, Editions du Piat, Glavenas, 43200 Saint-Julien-du-Pinet, France

7. Pavia University, Italy

8. LGIT, CNRS, Université Joseph Fourier, Grenoble, France

9. LSCE, CEA-CNRS-UVSQ, Gif Sur Yvette, France

Manuscrit déposé le 7 juillet 2008; accepté après révision le 22 juillet 2009.

Les veines sont de deux types : (i) les plus anciennes, faiblement minéralisées (chlorite et épidote), sont horizontales à faiblement inclinées. Les fibres de quartz (= direction d'extension) sont toujours verticales ; (ii) les plus récentes, très riches en minéraux (anatase, rutile, phénacite, meneghinite, beryl, synchysite, ...), sont verticales et leur disposition "en échelon" ainsi que les fibres de quartz horizontales qu'elles contiennent, indiquent un régime décrochant dextre.

Les âges Th-Pb se répartissent en deux groupes – 11 à 10 Ma et 7 à 5 Ma qui correspondent aux veines verticales, les plus récentes, mais échantillonnées dans des domaines différents du massif. Les âges voisins de 10 Ma correspondent à des veines ouvertes dans le granite de la Lauzière et son encaissant à environ 2 km du contact oriental du massif, tandis que les âges voisins de 5 Ma proviennent de veines situées dans les mylonites qui jalonnent ce contact. Les âges Ar/Ar des adulaires sont moins précis mais voisins de 7 Ma. Par ailleurs, nous avons aussi daté une monazite d'une veine du massif du Pelvoux (Plan du Lac) qui a fourni un âge Th-Pb de 17.6 Ma mais dans un contexte structural différent, encore mal connu pour l'instant.

En dehors des âges traces de fission, il n'y a que très peu d'âges de cet ordre dans la littérature récente concernant les Alpes. Ils concernent toujours des veines minéralisées en or (NE du Mont Blanc et SW du dôme lépontin). La dernière tectonique en compression datée entre 15 et 12 Ma correspond (i) au jeu du « Roselend thrust » [Ceriani *et al.*, 2001], dernier rejeu chevauchant du « Front pennique » qui se traduit dans le massif du Mont Blanc par des zones de cisaillement à linéation verticale ; (ii) à la fin du mouvement dans les mylonites basales des nappes helvétiques ; (iii) aux fentes alpines du Mont Blanc (veines horizontales et à fibres de quartz verticales) similaires aux veines précoces de la Lauzière. Au contraire, les veines verticales de la Lauzière, datées entre 11 et 5 Ma, correspondent à un régime en décrochement dextre. Cela suggère que l'essentiel de la tectonique en décrochement le long des MCE, a eu lieu en plusieurs étapes (ca. 10 Ma et ca. 7-5 Ma) et non pas vers 18 Ma comme cela avait été proposé précédemment.

L'ensemble des MCE était donc tectoniquement actif, en décrochement dextre pendant la crise messinienne.

The aim of this study is to document and to date the recent deformation and metamorphic events that affected the pre-Alpine basement of the External Alps, especially in one of the "External Crystalline Massifs" (ECM), the Lauzière massif. A recurrent problem for long in the external Alps is to find out good evidence for an Alpine rejuvenation of part of the Variscan pre-Alpine basement. Most authors consider that the behaviour of the pre-Alpine gneissic and granitic basement was passive except within restricted "lineaments" of retrogressive deformation along faults [e.g. Bordet and Bordet, 1963; Carme, 1971; Bellière, 1980; Von Raumer, 1984]. From a careful comparison of schistosity in basement and cover, Gourlay [1984] suggested that, in the Mont Blanc region, the Alpine deformation of the basement was significant. Evidence for an important Alpine imprint in the basement are coming out from recent papers on the Mont Blanc [Leloup *et al.*, 2005, 2007; Rolland *et al.*, 2003, 2007]. Besides the numerous geochronological data showing the Alpine age of shear zones in several massifs (see references in § Geochronology), the eastern part of the Lauzière massif provides unequivocal structural evidence for a ductile deformation and Alpine metamorphism superimposed on older Variscan structures since Stephanian conglomerates are involved in the deformation. Direct dating of the Alpine metamorphism affecting the ECM has never been successful and an indirect approach is necessary. The discovery of uranium, thorium and potassium-bearing minerals (monazite and adularia) in quartz veins, described in a special issue of the journal "Le Règne minéral" [de Ascencao Guedes, 2000] was an opportunity to try dating the last stages of the Alpine evolution of the massif and to characterize the structural setting of the veins and their relationships with a possible Alpine ductile deformation. The modalities of hydrothermal activity operating during the vein formation will not be discussed in this paper. Readers may refer to Rolland *et al.* [2003] and Rossi [2005] for a study of hydrothermal activity in the Mont Blanc massif.

GEOLOGICAL SETTING

The Lauzière massif belongs to the ECM that form the pre-Alpine basement of the "Helvetic" (or "Dauphinois") domain, the westernmost paleogeographic domain of western Alps and constitutes the northern prolongation of the Belledonne massif. Before Triassic times, ECM were part of the post-Variscan European platform located to the west of the future Tethys ocean. The Lauzière massif is formed by Variscan metamorphic rocks and granites but does not include late-Variscan granites (ca. 300 Ma) as in the Mont Blanc massif. The autochthonous Mesozoic cover is not preserved but some remnants may be found nearby, in the Beaufortain area to the north, and in the Grand Arc to the west. However, a deformed Carboniferous formation is exposed along the eastern flank of the Lauzière Massif.

On both western and eastern sides of the massif, deformed Triassic and Liassic formations of the Dauphinois domain occur. The western contact is an Alpine tectonic zone, the Median Fault (MF), that can be followed from the south of Belledonne near Grenoble, to the Beaufortain massif (fig. 1) and is outlined by a discontinuous strip of Mesozoic rocks. The MF was interpreted as a NE-trending dextral strike-slip deformation belt [Hubbard and Mancktelow, 1992]. Along the eastern contact of the Lauzière Massif, the Alpine deformation is more pervasive (Villard Benoît and Bonneval Formations, see below) and was often qualified as mylonitic. This contact corresponds to a major fault, the Ornon-Roselend fault that can be followed all along the Belledonne ECM and marks the eastern flank of the massif. The fault is vertical along most of its length but becomes E-dipping in the Beaufortain and in the SW part of the Mont Blanc Massif.

In between Arc and Isère valleys, the Lauzière massif consists of several lithological units, parallel to its NE-SW elongation [Poncerry, 1981; De Ascencao Guedes and Goujou, 2000]. These are, from NW to SE (fig. 2):

- the Epierre granite, a northern prolongation of the Sept Laux granite in the Belledonne massif, a high-K calc-alkaline, magnesian pluton dated at 335 +/-13 Ma [Debon *et al.*, 1998; Debon and Lemmet, 1999];
- a formation of gneisses, micaschists, leptynites, and migmatites corresponding to the Série Brune or Saint Remy Group defined by Bordet and Bordet [1963] and Gasquet [1979] respectively;
- a formation of greenschists and amphibolites, of probable Devonian to Tournaisian age, rich in subhorizontal sulfide-bearing veins;
- a complex of migmatized orthogneisses of pre- to early Variscan age, also including micaschists and granodiorites (the Colomban complex defined by Poncerry [1981]);
- the Lauzière monzogranite, which intrudes the Colomban micaschists and was dated at 341 +/-13 Ma [Debon *et al.*, 1998];
- a formation of gneisses, amphibolites and leptynites (Montagne des Plans formation), which has been compared to the classical leptyno-amphibolic complex from French Massif Central, and which is intruded by the Lauzière monzogranite;
- the Villard Benoît formation, a post-Variscan detrital formation that contains sandstones, conglomerates and black schists of Lower Stephanian age. It was dated by *Pecopteris cyathea*, SCHLOTH. and *Sphenophyllum oblongifolium*, GERM. [Barfély *et al.*, 1984; De Ascensão Guedes, 1997] near the Col de la Madeleine;

- a mylonitic formation (the Bonneval formation) where deformed Variscan gneisses, micaschists and leptynites are interleaved with the Villard Benoît conglomerates.

Tectonic and metamorphic fabrics observed in the Villard Benoît Formation have been used as references to distinguish the Alpine and pre-Alpine textures and mineral assemblages observed in the other formations. At first view, the Alpine deformation does not appear to be pervasive but is localized within lineaments that parallel Alpine (or rejuvenated pre-Alpine) dextral faults. The overall pattern of such faults is viewed as the imprint of the Alpine-scale Neogene convergence [Hubbard and Mancktelow, 1992]. In between the lineaments, the Alpine deformation is very weak.

For further comparison a sample of monazite from a quartz vein from the Plan du Lac area, in the Pelvoux massif (about 60 km South of the Lauzière), an area where monazite-bearing quartz veins are known for long, was included in this study. The corresponding structural pattern shows many similarities with the Lauzière. Close to a major fault (the Herpie fault, well known in the Grande Rousses massif further north), which is flanked by a narrow graben of deformed Stephanian schists and conglomerates, quartz veins of Plan du Lac occur within a km-wide north-south trending belt of heterogeneous Alpine deformation. The veins are flat lying and contain vertical quartz fibres. They occur within large competent boudins of leucocratic fine-grained gneisses enclosed in north-south trending

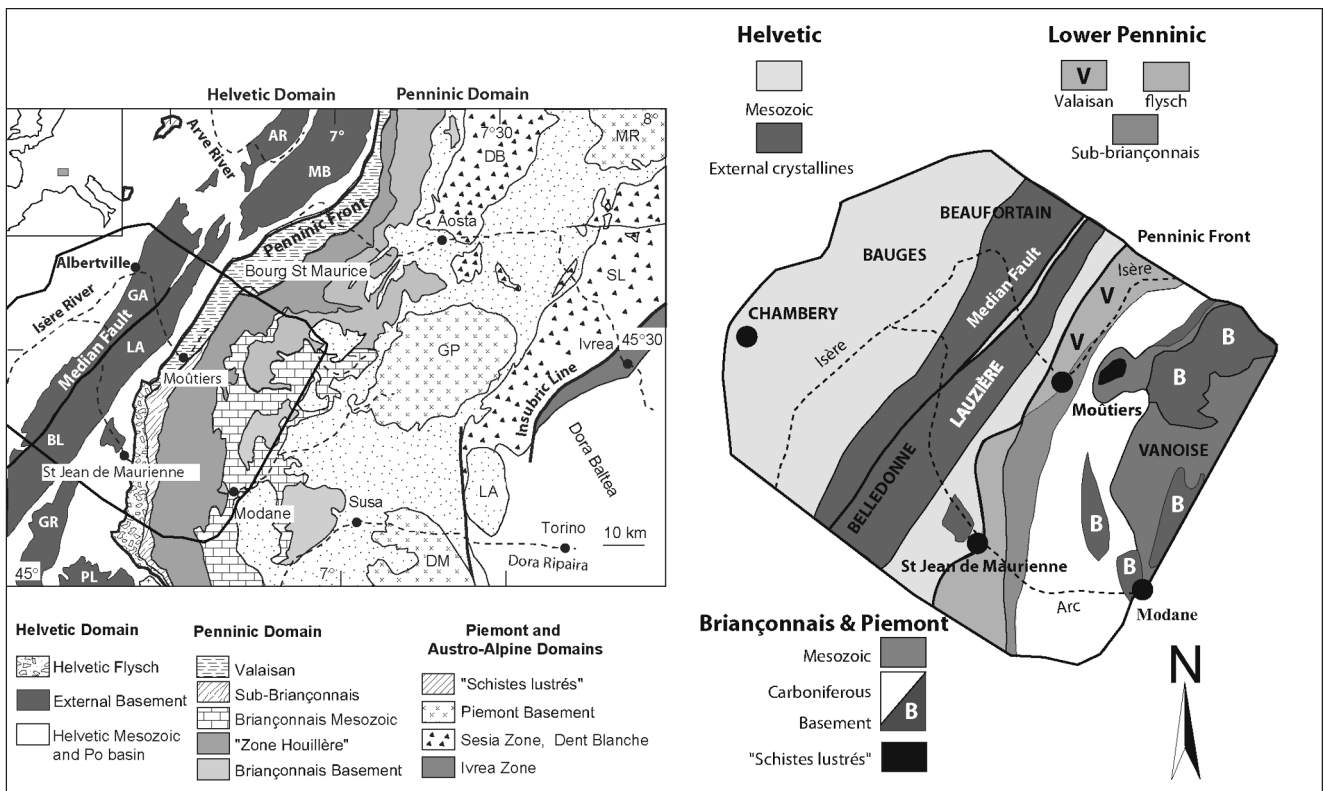


FIG. 1. – Geological setting of the Lauzière massif in the western Alps. Abbreviations : AR, Aiguilles Rouges; MB, Mont Blanc; GA, Grand Arc; LA, Lauzière; BL, Belledonne; GR, Grandes Rousses; PL, Pelvoux; ZHB, Zone Houillère Briançonnaise; GP, Gran Paradiso; DB, Dent Blanche; MR, Monte Rosa; SL, Sesia-Lanzo; LA, Lanzo massif; DM, Dora Maira.
 FIG. 1. – Cadre géologique du massif de la Lauzière.

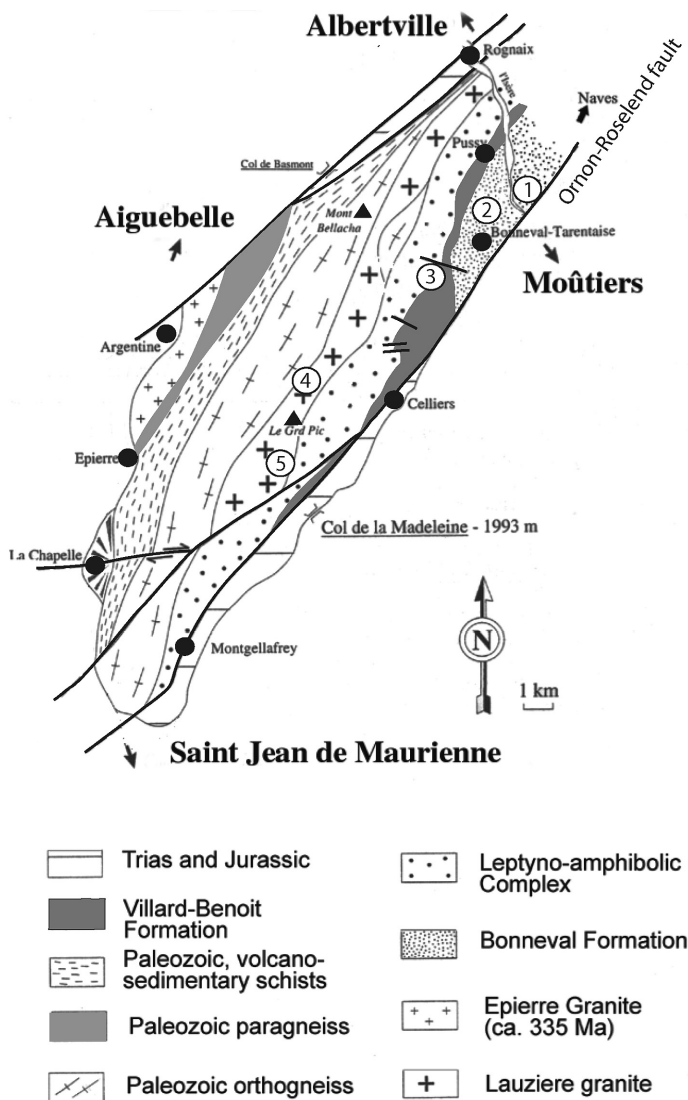


FIG. 2. – Sketch map showing the main geological units forming the Lauzière massif.

FIG. 2. – Carte schématique des principales unités géologiques du massif de la Lauzière.

retrogressed schists very similar to those of the Bonneval mylonitic formation defined in the Lauzière region. It is tempting to compare the Plan du Lac quartz veins and retrogressed schistosity with the Lauzière flat-lying veins and S2 schistosity, but a detailed study of the area has still to be done.

RELATIVE CHRONOLOGY OF DUCTILE EVENTS

In order to unravel the significance of the quartz veins and to establish a relative chronology for the Alpine events, our field work was focused on two areas in the Bonneval formation [Lehmann, 2004; Ratzov, 2004]: along the Naves road and near Bonneval-Tarentaise (fig. 2, areas 1 and 2) with surveys in the Villard Benoît and Montagne des Plans formations (areas 3, 4) and in the Lauzière granite (area 5).

At the Naves and Bonneval road sites (areas 1 and 2 on fig. 2) and in the Villard Benoît conglomerates (area 3), the relative chronology established from field and microscopic observations is as follows:

- a pre-Alpine migmatitic banding and foliation is outlined by flakes of large biotite (VBt, fig. 3A) and by deformed quartz and aplitic-pegmatitic veins. Relict pre-Alpine retrogressed alumina silicates (kyanite pseudomorphs?) were locally observed in the Bonneval Formation [De Ascensão Guedes, 1997];

- a low-grade, N010 to N030°E trending, vertical schistosity (S1) is well-defined in the Carboniferous rocks [De Ascensão Guedes and Goujou, 2000]. A conspicuous subhorizontal stretching lineation indicates, together with the vertical attitude of the schistosity, a WNW-ESE compression with a N010 to N030E-directed σ_3 . During this deformation event, tiny biotite recrystallized from pre-existing larger biotite (aBt, fig. 3A). This event corresponds either to a complete replacement or to re-crystallization within tension gashes especially in the Bonneval micaschists;

- a dissolution schistosity (S2) is superimposed upon the above structures and strikes N022°E 57 W. This younger schistosity is marked by alignments of chlorite and sericite crystals (fig. 3B). In the Bonneval Formation, the dissolution schistosity is almost parallel to the earlier low-grade schistosity. Near the eastern contact (area 1), the two schistosities are not easily distinguished on outcrops but are well observed in thin section (fig. 3C).

In the other Upper Carboniferous basins of the central Variscan belt (namely in the French Massif Central), there is no mention in the literature of the existence of a penetrative schistosity. Indeed, Stephanian deposits are usually localized in half grabens formed at high level during the late extensional event of the Variscan orogenic belt [Ledru *et al.*, 2001]. Even if pre-Triassic folding exists in some case (Alès basin), metamorphic minerals such as biotite have never been described. Therefore, we propose that the low-grade biotite-bearing S1 schistosity developed in the Lauzière Stephanian conglomerates results from the oldest Alpine event affecting the ECM region.

VEINS AND QUARTZ FIBRES

Two groups of quartz veins were observed (fig. 4):

- flat-lying or gently-dipping veins (fig. 4 A,B) are probably synchronous with the dissolution schistosity. As shown on the diagram all the quartz fibres are near-vertical whatever the dip of the vein (fig. 5);

- vertical veins are late and cross-cut all previous structures, including the dissolution schistosity. In area 1, the veins have a typical en-echelon habitus (fig. 4C) with sigmoidal, near-horizontal fibres indicating a dextral movement with respect to the direction of the basement-Lias contact. The angle of about 10° between the average vein direction and the basement contact, here parallel to a composite schistosity S1 + S2, suggests a dextral transpressive tectonic regime.

Flat-lying veins are dominant in the Bonneval road area (area 2) but vertical veins characterize the Naves road outcrops (area 1, fig. 4D), close to the eastern contact of the

basement. In the Lauzière granite (Branlay Lac, area 4), the vein pattern is similar to that of the Bonneval site. Nearly horizontal veins (up to 25-30°W dip) are dominant, but nearly vertical “en echelon” veins also occur (Entre-deux-Roches, area 5). Our samples from Entre-deux-Roches (area 5) correspond to these vertical veins. In area 4 (Branlay lake) late quartz veins crosscut obliquely the flat-lying veins and are characterized by boudinage and by roughly vertical thick quartz crystals rather than thin fibres.

Their relationships with the vertical en echelon veins observed elsewhere are unknown.

From our observations, the relationships between veins and Alpine schistosity are only clear in the case of the vertical veins that crosscut all pre-existing structures (S1 and S2). No direct relation has been observed between horizontal veins and S2. In the Lauzière massif there is no schistosity when flat-lying veins exist and where the S2 schistosity is developed, these veins do not exist. However, both S2 and flat-lying veins correspond to a similar kinematic regime (horizontal compression, vertical extension). The case is somewhat different in the Plan du Lac area (Pelvoux massif) where flat-lying veins and a retrogressed schistosity are clearly related and indicate a similar kinematic regime.

HYDROTHERMAL MINERALS

Dominant minerals found in both vertical and flat-lying veins are quartz, chlorite (Fe-clinocllore) ± epidote and albite. This assemblage is clearly hydrothermal in origin as shown by Poty [1969]. Flat-lying veins are characterized by chlorite + green epidote + calcite + sulfides, whereas vertical veins contain numerous species of rare minerals (see below).

In the horizontal veins, mineral assemblages seem to be broadly controlled by the composition of the surrounding lithologies. This feature and the presence of recurrent episyenitic dissolution halos surrounding veins suggest, even if fluids are exotic in origin, a local contamination.

P-T conditions were not studied for the Lauzière quartz veins. In the Mont Blanc massif, fluid inclusion thermometry from quartz [Poty *et al.*, 1974] and thermodynamic estimates from chlorites [Rossi *et al.*, 2003] indicate hydrothermal fluid temperatures of 350-400°C in accordance with the occurrence of sulphides in the horizontal veins, for a pressure of 3-4 kb.

Lead isotopic composition of three pure galena sampled from flat-lying veins are close to 18.60 ($^{206}\text{Pb}/^{204}\text{Pb}$ ratio)

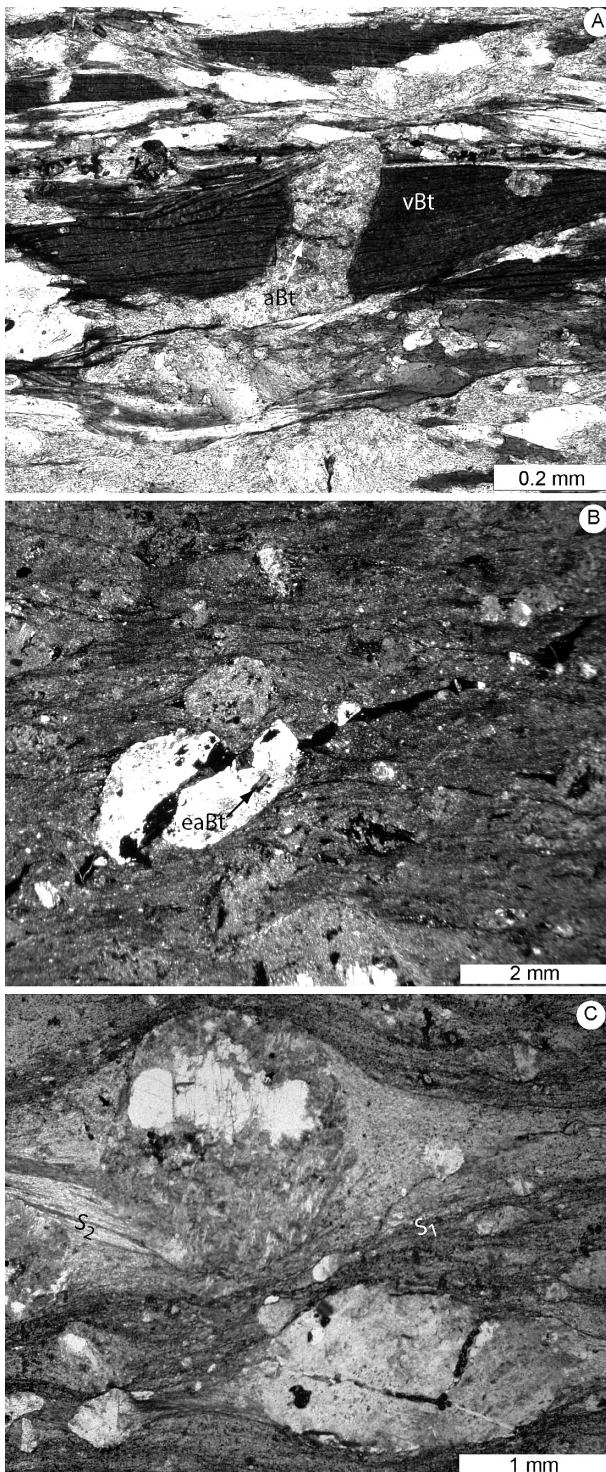


FIG. 3. – Microphotographs showing the deformation and recrystallisations in the Bonneval and Villar-Benoît formations. A: Bonneval-Tarentaise (area 2), broken old Variscan biotite (vBt) with recrystallisation of Alpine micro-biotite (aBt) in the tension gash. Another biotite crystal (bottom) is completely replaced by Alpine micro-biotite. B: Torrent du Tarlet (area 3). XZ section of a micro-conglomerate of the Villar-Benoît Formation: early alpine rotational deformation with recrystallisation of micro-biotite in the schistosity. Flakes of pre-Alpine biotite (eaBt) are preserved in the quartz clast. C: Bonneval (area 2), mylonite of the Bonneval Formation; the two Alpine schistosity are nearly parallel, S1 being outlined by micro-biotite. The younger schistosity (S2) is marked by sericite and oxides.

FIG. 3. – Déformation et recrystallisations à l'échelle microscopique dans les formations de Bonneval et de Villar-Benoît. A : Bonneval-Tarentaise (affleurement 2), ancienne biotite varisque fracturée (vBt) montrant une recrystallisation de néobiotite alpine dans la fracture (aBt). Un autre cristal ancien (bas de la photographie) est complètement remplacé par de la micro-biotite. B : torrent du Tarlet (affleurement 3). Section XZ section d'un microconglomérat de la formation de Villar-Benoît montrant une déformation rotationnelle alpine précoce et la recrystallisation de micro-biotite dans la schistosité. Des cristaux de biotite anté-alpine sont préservés dans le claste de quartz. C : Bonneval (affleurement 2), mylonite typique de la formation de Bonneval ; les deux schistosités alpines sont presque parallèles, mais S1 est soulignée par de la micro-biotite. La schistosité la plus jeune (S2) est marquée par de la séricite et des oxydes.

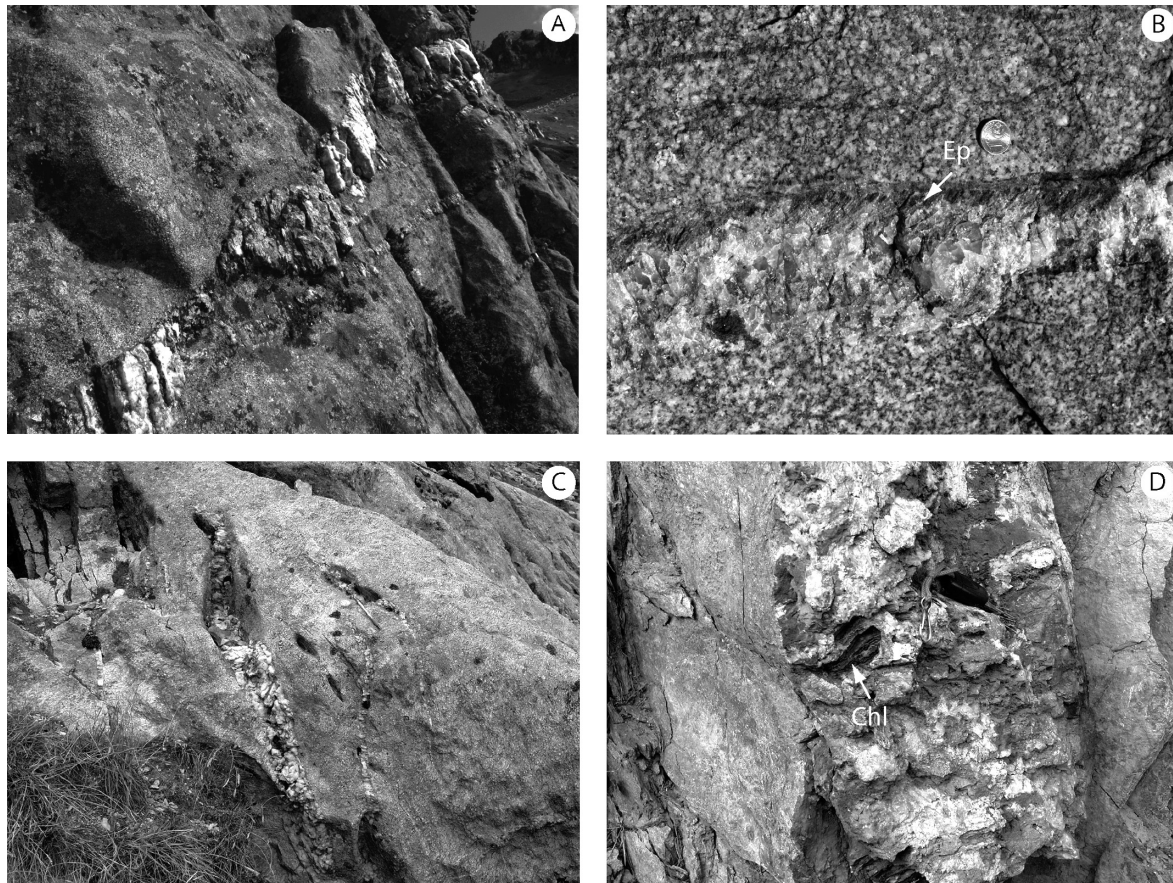


FIG. 4. – Quartz veins. A: Branlay lake (area 4), several flat-lying quartz + epidote veins cross-cut by a later flexuous and oblique veins with large quartz crystals. B: Branlay lake (area 4), detail of a flat-lying quartz + epidote vein. Epidote (Ep) crystallised as sub-vertical fibres. C: Entre-deux-Roches (area 5), an echelon quartz vein. D: Naves road (area 1), vertical vein with chlorite (Chl) and calcite showing flexuous sub-horizontal fibres.

FIG. 4. – Veines de quartz. A : lac de Branlay (affleurement 4), plusieurs veines de quartz + épidote de faible pendage sont recoupées par une veine plus tardive, flexueuse, formée de grands cristaux de quartz. B : lac de Branlay (affleurement 4), détail d'une veine de quartz + épidote à faible pendage. L'épidote (Ep) a cristallisé en fibres sub-verticales. C : Entre-deux-Roches (affleurement 5), veines de quartz en échelon. D : route de Naves (affleurement 1), veine de quartz verticale à chlorite (Chl) et calcite montrant des fibres flexueuses sub-horizontales.

and 15.65 ($^{207}\text{Pb}/^{204}\text{Pb}$ ratio) (table I). Using the Stacey and Kramers [1975] model, these isotopic compositions give μ ($^{206}\text{U}/^{204}\text{Pb}$) ratios of 9.62 (with an assumed age of 10 Ma). These values clearly locate the Pb source in the continental crust.

A wide range of mineralogical species (compiled by one of us – R. de A.G.) has been collected in the Lauzière massif by amateur mineralogists from various rock types:

– in amphibolites: adularia, epidote/clinozoizite, quartz, actinolite-tremolite, chlorite, calcite, pyrrhotite, pyrite, chalcocopyrite...

– in leucocratic gneisses: adularia, albite, calcite, allanite, anatase, rutile, brookite, ilmenite, quartz, chlorite, apatite, monazite...

– in granites close to the eastern contact: anatase, rutile, brookite, ilmenite, titanite, epidote, quartz, chlorite, blue beryl, bazzite, phenacite, meneghinite, pyrrhotite, pyrite, chalcocopyrite, calcite...

– in the Lauzière granite: red anatase, rutile, brookite, ilmenite, titanite, quartz crichtonite, epidote, chlorite, blue beryl, bertrandite, phenacite, Ce-synchysite, heulandite, stilbite, galena, chabazite...

– in the retrogressed gneisses and micaschists of the Bonneval Formation: adularia, albite, anatase, monazite, rutile, ilmenite, titanite, epidote, allanite, quartz, chlorite, Y-aeschynite, apatite, calcite...

– in the metasediments of the Villard Benoît Formation: gold in black schists, magnetite...

TABLE I. – ICP-MS Pb isotopes data of galena from Alpine veins of the Arc-Isère EDF gallery (see localization in Gasquet [1979]). The analyses were performed at the SARM-CRPG (Nancy) laboratory following procedures described by Carignan *et al.* [2001].

TABL. I. – Données isotopiques du plomb (ICP-MS) obtenues sur des galènes de veines de quartz de la galerie EDF Arc-Isère (voir localisation in Gasquet [1979]). Les analyses ont été réalisées au laboratoire SARM-CRPG (Nancy) selon les procédures décrites par Carignan *et al.*, [2001].

Sample	208/206 Pb	206/207 Pb	207/206 Pb	208/204 Pb	207/204 Pb	206/204 Pb
A828	2.0850	1.1818	0.8462	38.607	15.668	18.516
A1361	2.0771	1.1877	0.8420	38.580	15.639	18.574
A1020	2.0562	1.1947	0.8370	38.492	15.669	18.720
A1020-bis	2.0544	1.1954	0.8366	38.416	15.643	18.699
A1020-moyen	2.0553	1.1950	0.8368	38.454	15.656	18.709
Std Pb 250ppb / TI 25ppb	2.1676	1.0931	0.9148	36.722	15.498	16.942
sigma (n= 18)	0.0001	0.0002	0.0002	0.0091	0.0002	0.0035
References values [Thirlwall, 2002]	2.1677		0.91483	36.722	15.498	16.941
	± 0.0002		± 0.00007	± 0.008	± 0.003	± 0.002

– in the mylonites of the strongly deformed Bonneval Formation along the eastern contact zone: adularia, albite, anatase, rutile, brookite, ilmenite, Y-aeschynite, quartz, chlorite, fluoro-apatite, monazite, xenotime, epidote/clinozoisite, ferro-axinite, pyrrhotite, galena, pyrite, chalcopyrite,....

GEOCHRONOLOGY

Due to the very low grade of metamorphism – most estimate yield PT conditions of ca. 350°C and 3.5 kb [e.g. Fabre *et al.*, 2002; Rossi, 2005] – the precise dating of the Alpine events in the ECM and their cover is a difficult task. A good inventory of available ages may be found in Leloup *et al.* [2005, Fig 8]. Among the published data, three age-groups may be defined: ca. 26.5 Ma – 20 Ma; ca. 15 Ma; ca. 10 Ma.

1. ca. 26.5 – 20 Ma = a main metamorphic event and major shortening event in the External domain?

Metamorphism of the argillaceous limestones of the Dauphinois Lias of Bourg d'Oisans has been dated at 26.5 Ma [Nziengui, 1993] by K/Ar on the < 2 µm whole rock fraction of the sediment. In the same region, Crouzet *et al.* [2001] derived a metamorphic age of ca. 24 Ma (more precisely corresponding to the onset of cooling) by comparing the global polarity time-scale [Huestis and Acton, 1997] with a thermo-paleomagnetic sequence defined from remanent magnetism. These ages are the best estimate for the metamorphism of the ECM cover.

Concerning ECM basement rocks, phengites from shear zones in the basement of the Argentera massif have been dated at 22.2 ± 0.3 Ma [Corsini *et al.*, 2004] – the shear zone is related to a SW-directed thrust occurring during a

major compressive event. In the Mont Blanc massif, Leloup *et al.* [2005] estimate the onset of uplift at ca. 22 Ma from ³⁹Ar/⁴⁰Ar ages on biotite (22.8 ± 0.6 and 22.4 ± 0.1 Ma). Concordant pitchblende from the Lauzière massif yielded a U-Pb age of 21 ± 0.4 Ma [Negga, 1984].

2. The ca. 15 Ma event

K/Ar on muscovite (15.2 to 13.4 Ma) and adularia (18.3 to 15.2 Ma) were dated from Alpine veins of the Mont Blanc [Leutwein *et al.*, 1970]. An age of 14.2 ± 0.6 Ma K/Ar was obtained on phengite from a flat-lying vein oriented N118E, 35°SW in the Arc-Isère EDF gallery [Gasquet, 1979]. White mica from a post-kinematic quartz-calcite vein within the basal thrust of the Diablerets Nappe, NW of Mont Blanc massif, are dated at 15.5 ± 0.4 Ma by ³⁹Ar/⁴⁰Ar [Crespo-Blanc *et al.*, 1995]. This age was interpreted as the end of fluid flow and tectonic transport along the shear zone. Kirschner *et al.* [1996] analyzed white mica from synkinematic mylonites in shear zones of the Morcles Nappe and have shown that the youngest steps of the staircase spectra, at ca. 15 Ma, correspond to the last crystallized (< 2 µm) mica at the end of the deformation. Phengites from four shear zones of the Mont Blanc massif have been dated by ³⁹Ar/⁴⁰Ar at 15.8 ± 0.2 Ma and 16.0 ± 0.2 for samples from the east of the massif, and a little older but less precise (ca. 18 Ma) for a sample from the west [Rolland *et al.*, 2008]. Furthermore, micas crystallizing during ductile greenschist-facies deformation from the Aar massif display 21-17 Ma K-Ar ages [Challandes *et al.*, 2008].

3. The ca 10 Ma event

Adularia in gold bearing veins of NE Mont Blanc massif were dated at 9.9 ± 1 Ma [Marshall *et al.*, 1998]. Ages of ca. 10 Ma are also quoted for the quartz veins of the SW part of the Lepontine dome – Crodo: 10.6 ± 0.3 Ma [Petke *et al.*, 1999]. They are in contrast with neighbouring gold bearing veins from the Penninic domain (Brusson, Monte Rosa) that are dated at ca 30 Ma, and are clearly related to the major Oligocene event which is unknown in the External Alps.

New U/Th/Pb results on monazite

Most results presented here were obtained in two areas located respectively close to the eastern contact of the Lauzière massif (area 1 on figure 1) and at about 2 km from the same contact in the Lauzière granite (area 5).

In a first attempt, seven samples of euhedral, pale yellow to colourless and mm-size crystals of monazite were analysed by IDTIMS in using the technique reported by Paquette and Pin [2001]. Results are shown in table II. ²⁰⁶Pb/²³⁸U ages cannot be used here because in such young minerals, excess ²⁰⁶Pb resulting from radioactive disequilibria in the decay chain of ²³⁸U is responsible for too old ages and reversely discordant Concordia plot. As the studied monazites are hydrothermal, it is difficult to quantify accurately the Th/U ratio of their source in order to estimate a ²⁰⁶Pb correction. Consequently, the ²⁰⁷Pb/²³⁵U is the only available chronometer but is rather imprecise because ²⁰⁷Pb content is extremely low (0.15% to 0.5% of the whole lead isotopes) and consequently very sensitive to common lead correction. The U/Pb ages given in table II are quoted

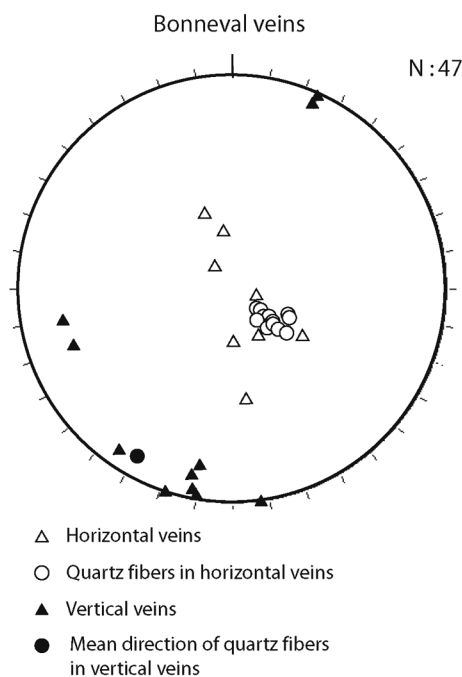


FIG. 5. – Stereograms of veins and quartz fibres from the Bonneval road area (area 2).

FIG. 5. – Stéréogramme des veines de quartz et de la direction des fibres, route de Bonneval (affleurement 2).

with large errors and are only indicative. Despite these poor precision, ages determined from different outcrops are similar within analytical errors and two major groups can be suggested at about 12 Ma and 7 Ma.

To constrain this first set of results, seven other monazite crystals from the same areas were analysed by LA-ICPMS in Pavia University to obtain $^{208}\text{Pb}/^{232}\text{Th}$ ages. $^{208}\text{Pb}/^{232}\text{Th}$ dating of young monazite using in situ techniques is a well established geochronological method [e.g. Harrison *et al.*, 1995; Stern and Sandborn, 1998] based on the high ^{232}Th content in most of the monazite crystals, which produces a significant amount of the daughter isotope ^{208}Pb in a very short time. Other advantages of the Th-Pb dating are the relative immobility of Th and the lack of long-lived intermediate daughter in the ^{232}Th - ^{208}Pb decay chain [Getty and DePaolo, 1995]. Each age, quoted at the 2σ level, is the average of 5 measurements on a single monazite grain (table II).

Analytical details of in-situ LA-ICPMS dating of monazite may be found in Paquette and Tiepolo [2007]. Spots of 25 μm wide were sampled using a 193 nm wavelength Geolas Pro Excimer laser coupled to a Thermo Element magnetic sector single collector ICP-MS. All fractionation effects were simultaneously corrected using a matrix-matched external standard [Tiepolo *et al.*, 2003; Jackson *et al.*, 2004]. In situ U-Th-Pb analyses closely depend to an external standard but there is no widely accepted standard to date. The Moacir monazite standard [Seydoux-Guillaume *et al.*, 2002] is a good candidate but needed to be re-calibrated. So, it was carefully dated by ID-TIMS using untreated fragments to avoid any Pb loss related to acid leaching during cleaning and a newly calibrated $^{205}\text{Pb}/^{235}\text{U}$ spike controlled by repeated mixing with Earthtime® gravimetric solutions. The calibration results are given here in order to validate our Alpine ages and to help the numerous users of this standard. In spite of its Cambrian age, the high Th content of the Moacir monazite (up to 7 wt.% ThO_2 according to Seydoux-Guillaume *et al.* [2004]) is responsible for the slight radioactive disequilibrium of the $^{206}\text{Pb}/^{238}\text{U}$ system and consequently of the reversely discordant behaviour of the analytical points in the Concordia diagram (fig. 6 and table III). Considering that

the $^{207}\text{Pb}/^{235}\text{U}$ ratio remains poorly disturbed by radioactive disequilibria in the U series [Schärer, 1984], a mean $^{207}\text{Pb}/^{235}\text{U}$ age of 504.3 ± 0.2 Ma is considered as the crystallisation time of the Moacir monazite. A reference $^{208}\text{Pb}/^{232}\text{Th}$ ratio of 0.02525 corresponding to 504.3 Ma is calculated accordingly and propagated into the data reduction using the software package Glitter® [Van Achtenberg *et al.*, 2001].

The occurrence of two groups of ages is confirmed by the in-situ $^{208}\text{Pb}/^{232}\text{Th}$ ages. The individual spots measured on EDR monazite grains indicate a weighted average $^{208}\text{Pb}/^{232}\text{Th}$ age of 11.6 ± 0.2 Ma. This first group is consistent with the ID-TIMS $^{207}\text{Pb}/^{235}\text{U}$ ages. LA-ICPMS analyses of the monazite samples (Mo samples on table II) spread over a larger period of time. Considering that MoG and MoB are comparable to MoE within error limits, a weighted average $^{208}\text{Pb}/^{232}\text{Th}$ age of 6.5 ± 0.5 Ma can be calculated. At the opposite, it may be argued that MoG sample is significantly younger than the others. A slight discordance or the occurrence of uncorrected common Pb into the monazite grain can explain this difference. In that case, a weighted average U-Th-Pb age of 7.1 ± 0.4 Ma is proposed. This latter age can be interpreted as the formation of the younger group of vertical veins.

Our comparative attempt to date a monazite far from the Lauzière massif – the Plan du Lac monazites in the Pelvoux massif – revealed an older $^{208}\text{Pb}/^{232}\text{Th}$ age at 17.6 ± 0.3 Ma, which does not fit, at first glance, with the Lauzière ages and will be dealt in the discussion. However, as the dated monazite occurs in flat-lying veins with vertical quartz fibres, this age provides a first insight to dating the major uplift of the ECM.

$^{40}\text{Ar}/^{39}\text{Ar}$ geochronology

Two samples of adularia from vertical veins cross-cutting the Bonneval formation (Les Combes and Bonneval Tarentaise, area 2) – LA-0501 (close to monazite sample MoE) and LA-0502 (close to monazite sample MoD) – have been dated by the $^{40}\text{Ar}/^{39}\text{Ar}$ method.

TABLE II. – Monazites ages from the Lauzière massif with a sample from Pelvoux massif for comparison.
TABL. II. – *Âges des monazites du massif de la Lauzière et d'un échantillon du massif du Pelvoux pour comparaison.*

Sample origin	Sample N°	Area	U ppm	Th ppm	$^{207}\text{Pb}/^{235}\text{U}$	$^{208}\text{Pb}/^{232}\text{Th}$	$^{207}\text{Pb}/^{235}\text{U}$	$^{208}\text{Pb}/^{232}\text{Th}$	Mean Pb/Th
					$\pm 2\text{ s error}$	$\pm 2\text{ s error}$	age (Ma)	age (Ma)	Age (Ma)
					IDTIMS	LA-ICPMS	LA-ICPMS	LA-ICPMS	LA-ICPMS
Entre-2-Roches	EDR1/1*	5	134	5920	0.0120 ± 36	0.000580 ± 9	12.1 ± 3.6	11.7 ± 0.2	
Entre-2-Roches	EDR1/2*	5	194	11515	0.0139 ± 42		13.9 ± 4.2		
Entre-2-Roches	EDR3	5	160	5140	0.0073 ± 21	0.000571 ± 37	7.4 ± 2.2	11.5 ± 0.7	
Entre-2-Roches	EDR4	5	206	4980	0.0094 ± 28	0.000556 ± 29	9.5 ± 2.8	11.3 ± 0.7	EDR : 11.6 ± 0.2
Les Combes	Mo E	near 2				0.000338 ± 48	6.3 ± 0.8	6.7 ± 0.9	
Bonneval-Tarentaise	Mo D/1*	2	31	2400	0.0076 ± 23		7.7 ± 2.3		
Bonneval-Tarentaise	Mo D2	2	35	3045	0.0072 ± 31		7.3 ± 3.2		
Naves road	Mo B	1				0.000356 ± 20		7.2 ± 0.4	Mo : 6.5 ± 0.5
Naves road	Mo G	1	89	3585	0.0055 ± 23		5.6 ± 2.6	5.4 ± 0.5	
St Christophe en Oisans (Plan du Lac)	Pdl					0.000869 ± 9		17.6 ± 0.3	

* different grains from the same vein

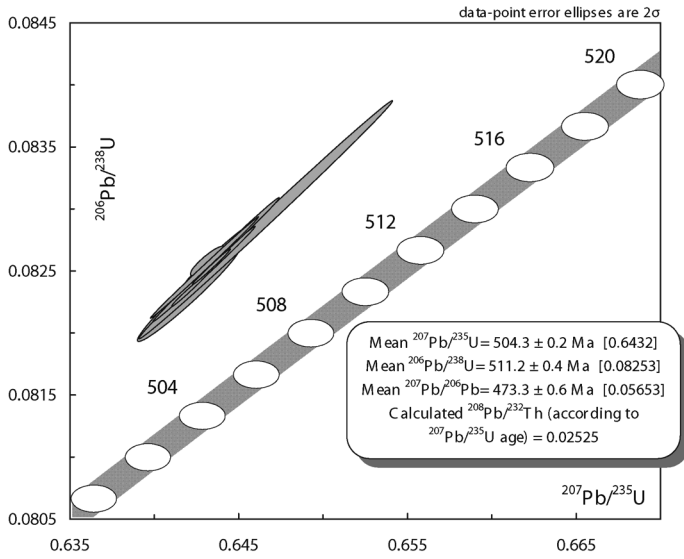


FIG. 6. – Concordia diagram of the Moacir standard.
 FIG. 6. – Diagramme Concordia du standard de Moacir.

40Ar/39Ar technique

Small (< 250 μm), translucent splinters were obtained from the coarse adularias sample LA-0501 and LA-0502 with tweezers under a binocular microscope. They were ultrasonically rinsed in deionized water, acetone, alcohol, and deionized water again. The mineral grains were loaded into two 4 mm ID separate holes on an Al-tray (with FC-sanidine as a flux monitor in three adjacent holes), and were irradiated for 1.5 hr in the central position of the Osiris reactor (CEA-Saclay, France). Calibration of the neutron flux received by the samples yielded a *J* factor of 6.58 (± 2.8%, 2 σ) 10⁻⁴.

Upon reception and cooling after irradiation, the adularia grains were transferred on a Cu-planchet machined with 4 mm ID holes, each loaded with one crystal from each

sample. The grains were degassed in several consecutive steps at increasing laser power using a 20 W SYNRAD CO₂ laser source until fusion of the sample. The gas were purified by exposure to a GP50 non-evaporable getter pump equipped with a St101 cartridge operated at 225°C, and a Ti-sublimation pump operated at room temperature before admission into a GV 5400 mass-spectrometer. Data reduction and analysis followed standard procedures described in detail elsewhere [Scaillet, 1996, 2000].

40Ar/39Ar results

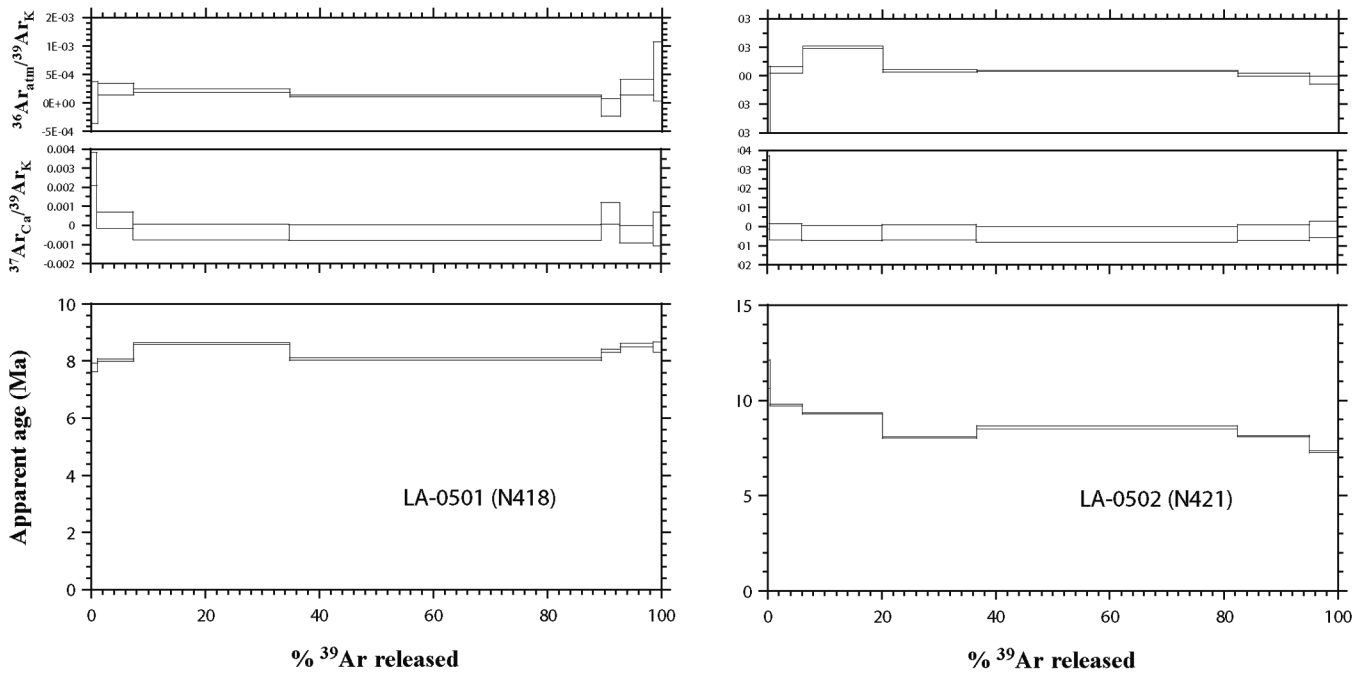
Both samples yielded rather complex degassing age patterns (fig. 7) with low-temperature ages initially decreasing from about 10 Ma to 8 Ma, then stabilizing around 8.5 Ma, further decreasing again to ca. 7.8 Ma in the fusion step for LA-0502. LA-0501 displays a slightly less complex, though still discordant, pattern with apparent ages mostly evolving around 8-9 Ma (but with a small age increase towards the final steps). These age variations are not mirrored by the ³⁷Ar_{Ca}/³⁹Ar_K and the ³⁶Ar_{atm}/³⁹Ar_K spectra, which are essentially homogeneous and tied to the bottom (zero) value. No age plateau can be calculated and the total-gas (integrated) ages are somewhat similar for both samples at 8.78 ± 0.26 Ma (LA-0501, 2σ) and 9.10 ± 0.26 Ma (LA-0502, 2 σ, table IV).

When reported in an inverse isochron plot (³⁶Ar_{atm}/⁴⁰Ar_{tot} vs. ³⁹Ar_K/⁴⁰Ar_{tot}, fig. 8), the data points of both samples are found to plot very near the abscissa due to their very high radiogenic yield (in excess of 98%). This prevented to obtain high-precision isochrons due to the moderate spread of the data points. Two colinear trends can be tentatively fitted to produce an age of 7.74 ± 2.8 Ma (2 σ) for LA-0501 (MSWD = 0.89) and 7.01 ± 0.74 Ma (2 σ) for LA-0502 (MSWD = 1.8, arbitrarily excluding the intermediate step #3). The (⁴⁰Ar/³⁶Ar)_{trapped} ratios projected from the linear fits are somewhat high with rather large errors due to the small spread of the data along the X-axis. Although admittedly the isochron data are far from ideal (little data spread, data tied to the abscissa, and one

TABLE III. – U-Pb data of Moacir standard
 TABL. III. – Données isotopiques U-Pb obtenues pour le standard de Moacir (monazite).

Analysed sample	Weight (μg)	U (ppm)	Pb rad (ppm)	²⁰⁶ Pb	²⁰⁸ Pb	²⁰⁶ Pb	²⁰⁷ Pb	²⁰⁷ Pb	²⁰⁶ Pb	²⁰⁷ Pb	²⁰⁷ Pb	
				²⁰⁴ Pb	²⁰⁶ Pb	²³⁸ U	²³⁵ U	²⁰⁶ Pb	²³⁸ U	²³⁵ U	²⁰⁶ Pb	²⁰⁶ Pb
concentrations				atomic ratios		ratios		apparents ages (Ma)				
MO 1	112	889	1325	2676	19.520	0.08280 (0.29)	0.6451 (0.29)	0.05650 (0.03)	512.8	505.5	472.2	
MO 2	99	879	1300	2934	19.489	0.08235 (0.14)	0.6420 (0.14)	0.05655 (0.02)	510.1	503.6	473.9	
MO 3	132	878	1304	3170	19.535	0.08253 (0.14)	0.6433 (0.15)	0.05653 (0.02)	511.2	504.3	473.3	
MO 4	93	1043	1517	3444	19.135	0.08247 (0.39)	0.6429 (0.39)	0.05653 (0.03)	510.9	504.1	473.4	
MO 5	185	1010	1513	3710	19.646	0.08291 (0.95)	0.6465 (0.96)	0.05655 (0.06)	513.5	506.3	474.2	
MO 6	157	1070	1593	3390	19.631	0.08246 (0.10)	0.6431 (0.10)	0.05656 (0.02)	510.8	504.2	474.4	
MO 7	133	1043	1549	3020	19.581	0.08230 (0.38)	0.6419 (0.39)	0.05657 (0.09)	509.9	503.5	474.7	
MO 8	183	1021	1534	3033	19.751	0.08262 (0.16)	0.6444 (0.15)	0.05657 (0.02)	511.7	505.0	474.7	
MO 9	160	984	1463	2598	19.543	0.08250 (0.14)	0.6430 (0.14)	0.05653 (0.02)	511.1	504.2	473.1	
MO 10	250	1058	1541	4717	19.164	0.08260 (0.11)	0.6434 (0.11)	0.05650 (0.02)	511.6	504.4	472.0	
MO 11	170	1008	1473	3882	19.201	0.08262 (0.22)	0.6435 (0.23)	0.05649 (0.03)	511.7	504.5	471.8	
MO 12	199	1032	1502	2862	19.102	0.08258 (0.12)	0.6431 (0.13)	0.05648 (0.06)	511.5	504.2	471.2	
MO 13	113	945	1495	3583	20.903	0.08252 (0.41)	0.6429 (0.41)	0.05650 (0.03)	511.1	504.1	472.2	

The isotopic ratios are corrected for mass discrimination (0.1 ± 0.015 % per amu for Pb and U), isotopic tracer contribution and analytical blanks: 6 pg for Pb and less than 1 pg for U. Initial common Pb is determined for each fraction in using the Stacey & Kramers [1975] two-step model. Absolute errors in percent are given at the 2σ level.

FIG. 7. – Step-heating $^{40}\text{Ar}/^{39}\text{Ar}$ results, samples LA-0301 and LA-0502.FIG. 7. – Résultats $^{40}\text{Ar}/^{39}\text{Ar}$ obtenus par chauffage par paliers, échantillons LA-0301 et LA-0502.

outlier for LA-0502), they give support to the presence of excess ^{40}Ar . Therefore, they suggest a probable common age around ca. 7 Ma for both samples when due account is taken for this excess component based on the regressed steps.

Based on the disturbed shape of the age spectra, the intracrystalline distribution of this excess component is very irregular and we surmise that the complex Ar/Ar systematics of both adularia samples are due to overlapping

Ar-reservoirs that are irregularly degassed during the stepheating experiments. Inhomogeneous decrepitation of ^{40}Ar excess-bearing fluids inclusions under the laser beam probably explains the complex spectrum shapes in both cases, though more exhaustive work would be needed to ascertain if there are more than one generation of fluid inclusions contributing to the Ar budget of these samples. On account of the above complications, we thus take the apparent ages of the stepheating data around 9 Ma as a maximum

TABLE IV. – $^{40}\text{Ar}/^{39}\text{Ar}$ data.TABL. IV. – Données isotopiques $^{40}\text{Ar}/^{39}\text{Ar}$.

Step # Spot #	$^{39}\text{Ar}_K$ (V)	$^{36}\text{Ar}_{\text{atm}}/^{39}\text{Ar}_K$ ($\pm 1\sigma$)	$^{37}\text{Ar}_{\text{Cr}}/^{39}\text{Ar}_K$ ($\pm 1\sigma$)	$^{38}\text{Ar}_{\text{Cr}}/^{39}\text{Ar}_K$ ($\pm 1\sigma$)	% $^{40}\text{Ar}^*$	$^{40}\text{Ar}^*/^{39}\text{Ar}_K$ ($\pm 1\sigma$)	Age (Ma) ($\pm 1\sigma$)
N418 LA-0501 (#1) (J = .6199E-03 \pm .1399E-04; total-gas age error includes the J error)							
# 1	7.54E-05	1.66E-05 \pm 3.68E-04	2.97E-03 \pm 8.69E-04	6.37E-04 \pm 2.50E-03	99.9	6.99 \pm 0.13	7.798 \pm 0.14
# 2	4.66E-04	2.48E-04 \pm 1.05E-04	2.91E-04 \pm 4.26E-04	-5.08E-04 \pm 2.49E-03	99.0	7.21 \pm 0.04	8.048 \pm 0.05
# 3	2.02E-03	2.17E-04 \pm 2.75E-05	-3.53E-04 \pm 4.09E-04	-1.83E-04 \pm 2.48E-03	99.2	7.73 \pm 0.03	8.623 \pm 0.03
# 4	4.03E-03	1.29E-04 \pm 1.88E-05	-3.81E-04 \pm 4.07E-04	-3.17E-04 \pm 2.48E-03	99.5	7.25 \pm 0.04	8.085 \pm 0.05
# 5	2.42E-04	-7.40E-05 \pm 1.52E-04	6.51E-04 \pm 5.61E-04	-5.57E-04 \pm 2.49E-03	100.3	7.50 \pm 0.06	8.371 \pm 0.07
# 6	4.29E-04	2.82E-04 \pm 1.32E-04	-4.48E-04 \pm 4.53E-04	3.81E-05 \pm 2.49E-03	98.9	7.68 \pm 0.05	8.572 \pm 0.05
# 7	1.10E-04	5.61E-04 \pm 5.16E-04	-1.66E-04 \pm 8.94E-04	-9.15E-04 \pm 2.50E-03	97.9	7.62 \pm 0.16	8.504 \pm 0.18
Total	7.37E-03	1.68E-04 \pm 1.91E-05	-2.64E-04 \pm 2.53E-04	-2.79E-04 \pm 1.54E-03	99.3	7.41 \pm 0.02	8.271 \pm 0.19
N421 LA-0502 (#1) (J = .6199E-03 \pm .1399E-04; total-gas age error includes the J error)							
# 1	4.87E-05	-1.93E-03 \pm 2.27E-03	1.82E-03 \pm 1.93E-03	-1.10E-03 \pm 2.57E-03	105.9	10.22 \pm 0.68	11.39 \pm 0.76
# 2	8.18E-04	2.16E-04 \pm 1.11E-04	-2.55E-04 \pm 4.22E-04	-6.05E-04 \pm 2.49E-03	99.3	8.76 \pm 0.04	9.77 \pm 0.05
# 3	2.03E-03	1.01E-03 \pm 4.63E-05	-3.21E-04 \pm 4.08E-04	-6.57E-04 \pm 2.48E-03	96.5	8.36 \pm 0.04	9.32 \pm 0.04
# 4	2.38E-03	1.87E-04 \pm 3.94E-05	-2.92E-04 \pm 4.08E-04	-5.05E-04 \pm 2.48E-03	99.2	7.22 \pm 0.03	8.06 \pm 0.03
# 5	6.59E-03	1.97E-04 \pm 1.67E-05	-3.88E-04 \pm 4.07E-04	-5.10E-04 \pm 2.48E-03	99.3	7.71 \pm 0.08	8.60 \pm 0.08
# 6	1.82E-03	5.02E-05 \pm 6.09E-05	-3.07E-04 \pm 4.11E-04	-3.48E-04 \pm 2.48E-03	99.8	7.30 \pm 0.03	8.14 \pm 0.03
# 7	7.26E-04	-1.38E-04 \pm 1.50E-04	-1.48E-04 \pm 4.27E-04	-4.53E-04 \pm 2.49E-03	100.6	6.54 \pm 0.05	7.30 \pm 0.05
Total	1.44E-02	2.69E-04 \pm 1.89E-05	-3.25E-04 \pm 2.15E-04	-5.14E-04 \pm 1.31E-03	99.0	7.68 \pm 0.04	8.56 \pm 0.20

age for both samples, and tentatively regard the 7.0 ± 0.74 Ma isochron age as a best excess-corrected estimate (based on sample LA-0502) until more Ar/Ar data can be obtained on these (or other related) hydrothermal veins.

DISCUSSION AND CONCLUSIONS

Disputed for long, a clear recognition of Alpine fabrics, microtextures and mineral assemblages in the pre-Alpine basement of the External Alps is now possible, thanks to the discovery of Carboniferous floras in a clastic formation interleaved and deformed together with basement rocks [Barf  ty *et al.*, 1984; De Ascen  o Guedes, 1997]. As a consequence, the structures and mineral assemblages corresponding to the oldest Alpine event are now well-defined, even if still undated, in the Lauzi  re massif. They are superimposed on an older, Variscan mineral assemblage.

A chronology of the Alpine events in the Lauzi  re massif is proposed:

- a first WNW compressive deformation (S1 schistosity) is characterized by an horizontal extension (N010 to N030 stretching lineations) that corresponds to the main deformation in the Liassic formations surrounding the massif and was clearly registered in the detrital Villard Beno  t Formation (Late Carboniferous). This deformation is penetrative along the eastern contact (even at 2 km from the contact) but it is more spaced and less penetrative – or even absent – in the centre of the massif. Dated further south in the Liassic schists of Bourg d’Oisans at ca. 26 Ma [Nziengui, 1993], this schistosity is characterized by crystallisation of white mica, the corresponding PT conditions being still to be precised, but most authors agree for ca 350  C, 3-4 kb;

- an hydrothermal event that corresponds to differing kinematic conditions. A spaced, irregular dissolution

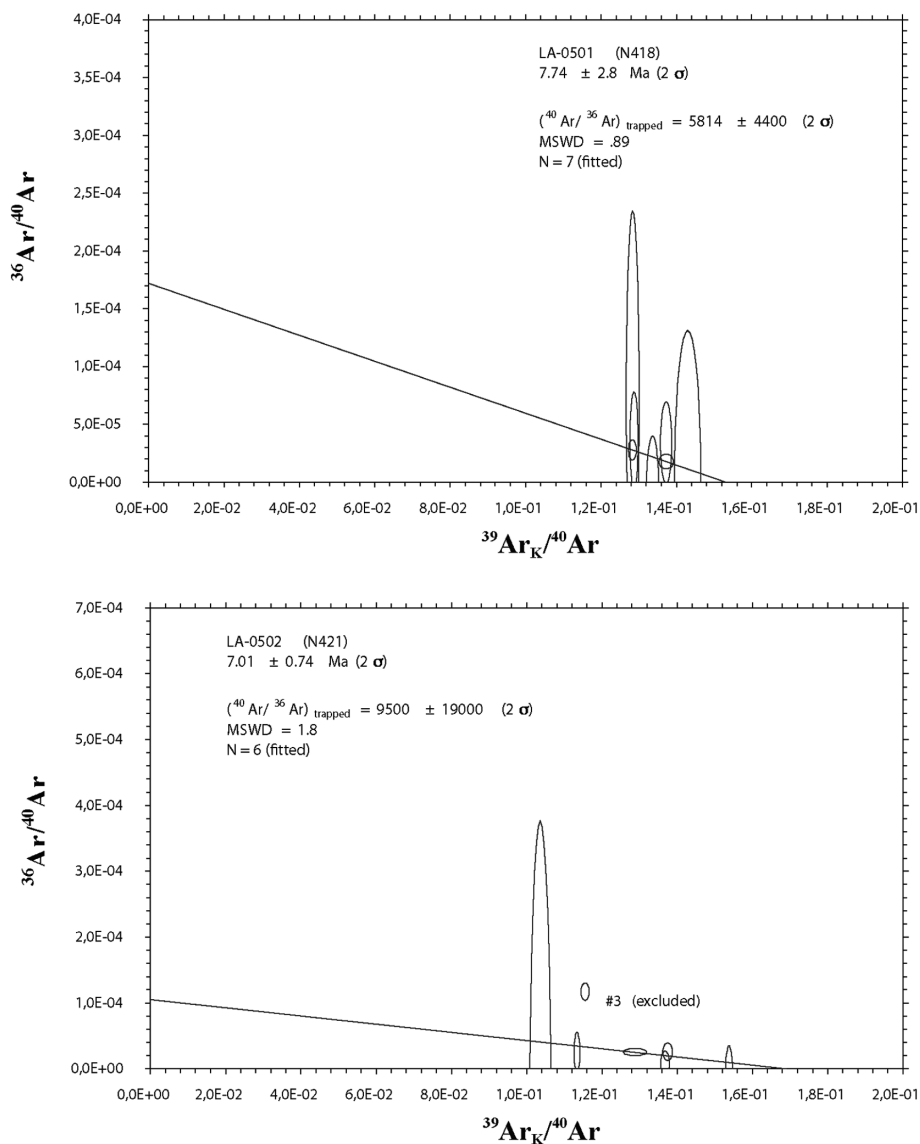


FIG. 8. – Argon isochron diagrams.

FIG. 8. – Diagrammes isochrones pour l’argon.

cleavage (S2) is probably coeval with near-horizontal quartz veins showing near-vertical fibres (σ 3 vertical). This stage is still undated but may correspond to the ca. 15 Ma old shear zones with vertical stretching lineations associated with horizontal veins in the Mont Blanc massif [Rossi, 2005; Rolland *et al.*, 2008]. We did not observe in Lauzière the shear zone pattern described in the Aar massif [Marquer, 1987; Choukroune and Gapais, 1983], and in the Mont Blanc massif [Rolland *et al.*, 2003; Rossi *et al.*, 2005]. An age of 14.2 ± 0.6 Ma (K/Ar on phengite) was obtained from a flat-lying vein oriented N118E, 35°SW in the Arc-Isère gallery [Gasquet, 1979] in the neighbouring Belledonne massif;

– the youngest stage corresponds to “en echelon” vertical quartz veins indicating a dextral movement along the main Ornon-Roselend fault. This orogen-parallel transpressive regime occurred in two separate pulses at 11 Ma and 7-5 Ma as evidenced by the crystallisation of monazite (and many other minerals) within the veins.

In the Alps, ages as young as 5.4 Ma have never been published so far for minerals related with a well-identified deformation event. The Lauzière monazites are too poor in U to allow precise U-Pb ages but fortunately much better Th-Pb ages were obtained in using ICPMS laser, that confirm and precise U-Pb ages. Argon ages on adularias, although less precise (poor plateaux with isochron ages of 6.6 ± 0.84 and 7.3 ± 2.8), broadly confirms the ages of the corresponding monazites. U-Th-Pb ages presented here suggest that two distinct hydrothermal pulses may be defined and correspond respectively to 11.7-11.3 Ma and 7.2-5.4 Ma ranges. Both are related to vertical veins with horizontal quartz fibres – and thus to a similar strike-slip tectonic regime. In the Lauzière area, hydrothermal activity occurred during, at least, two separate pulses at ca. 11 Ma and ca. 7-5 Ma. However, the number of pulses is not limitative at the ECM scale because, as shown in this study, the dated monazite from a quartz vein sampled in the Pelvoux massif (Plan du Lac, about 60 km to the south of the Lauzière), yielded an older age of 17.6 Ma. This implies that fluid circulation within shear zones and faults may have been diachronous at the scale of the ECM.

Tentative Neogene chronology in the External Alps

The Oligocene to Neogene tectonic evolution of western Alps is still not completely understood and many discrepancies remain regarding the chronology of events (table V). According to Ceriani *et al.* [2001], the Penninic Front (PF), immediately east of the ECM massifs, can be interpreted as a transpressive suture between the internal and external Alps. The internal Alps were deformed and metamorphosed before being sealed by the syntectonic deposition of the Ultrahelvetic flysch (Priabonian in age) along the PF. At the same time, the lower marine molasses of the Helvetic domain (external Alps) were deposited in the foreland basin [Schlunegger *et al.*, 2007]. An early normal faulting event occurred in the FP region at ca. 32 Ma [Ceriani *et al.*, 2001] and corresponds to the overall extensional regime prevailing during the lower Oligocene [Bergerat, 1987]. Ceriani *et al.* [2001] defined a “Roselend Thrust” that follows the PF along most of its length and was active from ca. 28 to 20 Ma. At that time the maximum burial and heating of the

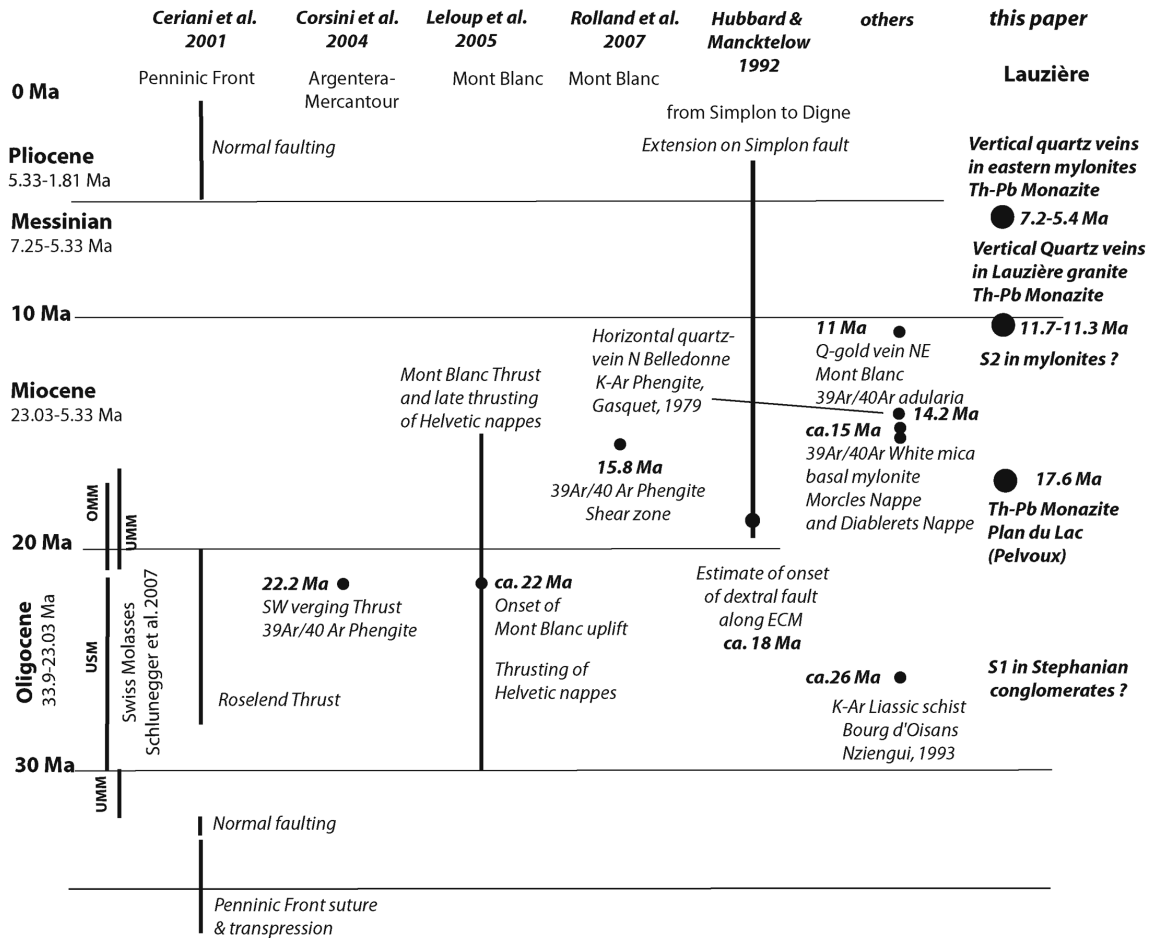
Mont Blanc and Belledonne massifs were reached as a result of underthrusting along the Roselend thrust.

In a recent paper, Leloup *et al.* [2005] described the shear zone pattern of the Mont Blanc and Aiguilles Rouges region. They propose that the Helvetic nappes were active between 30 and 15 Ma, the onset of uplift of the Mont Blanc being at ca. 22 Ma. The 15 Ma event corresponds to the end of motion along the basal thrusts of the Helvetic nappes [Crespo-Blanc *et al.*, 1995; Kirschner *et al.*, 1996]. After the end of emplacement of the Helvetic nappes, at 12 Ma, the Mont Blanc was overthrust with a dextral component and a total of 4 to 8 km of overthrow onto Aiguilles Rouges [Leloup *et al.*, 2005] along the Mont Blanc thrust (MBT). This thrust was active until 4 Ma as shown by fission track data. These ages are discussed by another group of workers [Rolland *et al.*, 2005; 2008] who claims that the dense network of shear zones (bearing vertical stretching lineations) that affects the Mont Blanc granite are 15 Ma old (Ar-Ar data) – the shear zones are associated with an intense hydrothermal activity and with the opening of flat-lying quartz veins filled with vertical quartz fibres similar to the situation described in this paper for the Lauzière set.

To reconcile these different interpretations with our data is not an easy task. Assuming that the Roselend thrust and the emplacement of the Helvetic nappes are broadly coeval, we suggest that the life for the Roselend thrust proposed by Ceriani *et al.* [2001] should be expanded to 15 Ma. Then the activity along the Roselend thrust might have lasted from 28 to 15 Ma the latter age being consistent with the presumed age of our S2 and horizontal veins. This time span also includes the 15 Ma shear zones (with flat-lying veins) in the Mont Blanc massif. We also refer to a phengite K-Ar age of 14.2 Ma from a flat-lying vein in the Belledonne massif [Gasquet, 1979]. Thus, taken together the Mont Blanc shear zones, the Belledonne veins and the Plan du Lac veins (at 17.6 Ma), indicate that the main uplift of the ECM occurred during the 18-14 Ma time range. However, nothing matches our S1 with its horizontal lineation suggesting an orogen-parallel extensional regime. Another misfit is the similarity between the 12 Ma age of the Mont Blanc thrust [Leloup *et al.*, 2005], a compressive event (with a dextral component however), and our purely transpressive en echelon vertical veins dated at 11 Ma that may also exist in Mont Blanc [Marshall *et al.*, 1996].

In most of the papers presented above, tectonic events occurring near the Miocene-Pliocene limit are only discussed from the fission tracks point of view, which mostly focuses on vertical movements. Our younger age group of 7-5 Ma is probably the first radiometric age that can be directly related to a deformation event. At the scale of the western Alps a dextral transpressive model [Hubbard and Mancktelow, 1992] integrates in a common kinematics the southward detachment along the Simplon fault, the strike-slip faults along and within the ECM and the westward Digne and Embrunais-Ubaye nappes emplacement. The proposed age of ca. 18 Ma [Hubbard and Mancktelow, 1992] for the onset of this transpressive is too old if compared with the now well-dated dextral deformation events recorded in the Lauzière, at 11 Ma and 7-5 Ma. Indeed if the Hubbard and Mancktelow model is accepted, our results (ca 11-7.5 Ma transpressive event) are consistent with the age of the last movements along the basal thrust of the

TABLE V. – A tentative Neogene comparative chronology.
 TABL. V. – Un essai de chronologie comparative des événements d'âge néogène.



Digne nappe which affects late Miocene to Pliocene formations [Gidon and Paris, 1992; Hippolyte *et al.*, 2008].

For the southern ECM, from Pelvoux to Argentera-Mercantour, structural and geochronological data dealing with the Alpine rejuvenation are scarce and difficult to compare with the Belledonne – Mont Blanc region. In the Pelvoux massif, our preliminary 17.6 Ma age on a monazite) from a flat-lying quartz vein is a possible link with the chronology proposed for the northern ECM and may help constraining the timing of the ECM uplift. In the Argentera massif, a 22 Ma old shear zone [Corsini *et al.*, 2004] is one of the first clearly Alpine event dated so far.

Messinian

Concerning the ca. 7-5 Ma age group, it appears that the youngest age is very close to the age of the Messinian event in the Mediterranean region. The onset of the “Messinian Salinity Crisis” is well dated at 5.96 Ma [Krijgsman *et al.*, 2002]. According to Schlunegger *et al.* [2007] the topographic axis of the Alpine belt (water divide) was located near the Insubric Line until the end of Miocene (5.33 Ma), and moved westward, toward the ECMs during the Pliocene. The crystalline core of the Internal Alps began to be exposed at the surface at ca. 20 Ma. Tectonic exhumation

of the Lepontine domain starts at about 28 Ma (peak of metamorphism) but exhumation rate decreases since 20 Ma. According to Willett *et al.* [2006], the Alps entered a constructional phase (accretionary flux > erosion flux) during the Middle Miocene, expanding to the north and to the south. The Miocene-Pliocene boundary marks a brutal arrest of deformation in the Jura, an arrest of the thrusts in Lombardy and the inversion and the erosion of the molassic basins. Then the Alps entered in a destruction phase probably related to a wetter climate during the Messinian [Willett *et al.*, 2001]. The end of deformation in the Jura corresponds to a backward displacement of the deformation front toward the ECM where fission track ages are very young and which shows evidences for recent deformation. It is difficult to further discuss the Messinian imprint on west Alpine morphologies because there is no (or very little) published data east to the Rhône Valley and Bas Dauphiné, probably because of the on-going uplift and erosion of the ECM. However, our study shows that in the Lauzière massif a well-dated tectonic activity occurred just before the Messinian event. The eastern edge of the ECM was a dextral fault at the same time, the Mediterranean Sea was emptying – from 5.96 Ma – or just before. Furthermore, evidence of hydrothermal activity with temperatures estimated at 350°C [Rossi, 2005] indicate that there is little

chance to find Messinian paleo-morphologies in the ECM regions because rocks that are now at the surface were deep-seated at that time – about 8-12 km, a maximum assuming a penetrative re-heating, not likely for hydrothermal activity, and using the today uplift rate of Belledonne of about 1.7 mm/y.

To conclude, this study shows: (i) that the Roselend thrust, which was estimated to have been active until 20 Ma [Ceriani *et al.*, 2001] was followed, between 18 Ma and 15 Ma by the main uplift of the ECM; (ii) evidence of major transpressive events associated with pulses of hot fluid circulation between 10 and 5 Ma, before the 5 Ma normal faulting suggested by FT data [Fügenschuh *et al.*, 1999], and not since 20 Ma as proposed by Hubbard and Mancktelow [1992] and (iii) that the last hydrothermal

pulse and associated dextral movement occurred at the same time or just before the Messinian salinity crisis that occurred further south.

Geochronological data presented in this paper are preliminary. A more complete study is now necessary at the scale of all the ECM and adularia would be easier to be found in the quartz veins than monazites. This is the reason why, even if argon data on adularia are less robust than Th/Pb ages on monazite, they are more promising for the future.

Acknowledgements. – This study was supported by a “BQR” grant (“Chronoréférencement”) of the University of Savoie. We would like to thank Valéry Ottone for sampling adularia and Y. Rolland, G. Ménard and M. Rossi for fruitful discussions. We also thank U. Schaltegger, Y. Lagabrielle and one anonymous reviewer for their constructive reviews.

SGF associate editor: Y. Lagabrielle.

References

- BARFÉTY J.-C., BLAISE J., FOURNEAUX J.-C. & MELOUX J. (1984). – Carte géologique de la France au 1/50 000, feuille La Rochette n° 750. – BRGM, Orléans France.
- BELLIÈRE J. (1980). – Massif du Mont Blanc et des Aiguilles Rouges, structure et pétrologie du socle. – *Géol. Alp.*, **56**, 237-249.
- BERGERAT F. (1987). – Stress fields in the European platform at the time of Africa-Eurasia collision. – *Tectonics*, **6**, 99-132.
- BORDET P. & BORDET C. (1963). – Belledonne-Grandes Rousses et Aiguilles Rouges-Mont Blanc: quelques données nouvelles sur leurs rapports structuraux. In: « Livre à la mémoire du Professeur P. Fallot ». – *Mém. h.s. Soc. géol. Fr.*, **II**, 309-320.
- CARIGNAN J., HILD P., MEVELLE G., MOREL J. & YEGHICHEYAN D. (2001). – Routine analyses of trace element in geological samples using flow injection and low pressure online liquid chromatography coupled to ICP-MS: a study of geochemical reference materials BR, DR-N, UB-N, AN-G and GH. – *Geostand. Newslett.*, **25**, 187-198.
- CARME F. (1971). – Les phases successives de déformation contenues dans l'ensemble Belledonne-Aiguilles Rouges (Massifs cristallins externes – Alpes françaises). – *C. R. Acad. Sci.*, Paris, **273**, 1771-1774.
- CERIANI S., FÜGENSCHUH B. & SCHMID S.M. (2001). – Multi-stage thrusting at the « Penninic Front » in the western Alps between Mont Blanc and Pelvoux massifs. – *Int. J. Earth Sciences*, **90**, 685-702.
- CHALLANDES N., MARQUER D. & VILLA I.M. (2008). – P-T-t modelling, fluid circulation, and $^{39}\text{Ar}/^{40}\text{Ar}$ and Rb-Sr mica ages in the Aar Massif shear zones (Swiss Alps). – *Swiss J. Geosci.* doi 10.1007/s00015-008-1260-6.
- CHOUKROUNE P. & GAPAIS D. (1983). – Strain pattern in the Aar granite (Central Alps): orthogneiss developed in inhomogeneous flattening. – *J. struct. geol.*, **5**, 411-418.
- CORSINI M., RUFFET G. & CABY R. (2004). – Alpine and late-Hercynian geochronological constraints in the Argentera Massif (western Alps). – *Eclogae Geol. Helv.*, **97**, 3-15.
- CRESPO-BLANC A., MASSON H., SHARP Z., COSCA M. & HUNZIKER J. (1995). – A stable and $^{40}\text{Ar}/^{39}\text{Ar}$ isotope study of a major thrust in the Helvetic nappes (Swiss Alps): evidence for fluid flow and constraints on the nappe kinematics. – *Geol. Soc. Amer. Bull.*, **107**, 1129-1144.
- CROUZET C., MÉNARD G. & ROCHETTE P. (2001). – Cooling history of the Dauphinoise Zone (western Alps, France) deduced from thermopaleomagnetic record: geodynamic implications. – *Tectonophysics*, **340**, 79-93.
- DE ASCENÇÃO GUEDES R. (1997). – Recherches structurales et cartographiques sur la série détritique mylonitisée de Villard-Benoit dans le secteur de La Léchère, Tarentaise, Savoie. – Mémoire Maîtrise, Université de Savoie.
- DE ASCENÇÃO GUEDES R. (2000). – Espèces minérales (Lauzière). – *Le Règne Minéral*, hors série **6**, 24-39.
- DE ASCENÇÃO GUEDES R. & GAUJOU J.-C. (2000). – Ce que disent les pierres de la Lauzière, les roches et les fentes à cristaux. – *Le Règne Minéral*, hors série **6**, 7-20.
- DEBON F., GUERROT C., MÉNOT R.-P., VIVIER G. & COCHERIE A. (1998). – Late Variscan granites of the Belledonne massif (French western Alps): an early Visean magnesium plutonism. – *Schweiz. Mineral. Petrogr. Mitt.*, **78**, 67-85.
- DEBON F. & LEMMET M. (1999). – Evolution of Mg/Fe ratios in Late Variscan plutonic rocks from the External Crystalline Massifs of the Alps (France, Italy, Switzerland). – *J. Petrol.*, **40**, 1151-1185.
- FABRE C., BOIRON M.C., DUBESSY J., CATHELINEAU M. & BANKS D.A. (2002). – Paleofluid chemistry of a single fluid event: a bulk and in-situ multi-technique analysis (LIBS, Raman spectroscopy) of an Alpine fluid (Mont-Blanc). – *Chem. Geol.*, **182**, 249-264.
- FÜGENSCHUH B., LOPRIENO A., CERIANI S. & SCHMID S.M. (1999). – Structural analysis of the Subbriançonnais units in the area of Moûtiers (Savoy, western Alps): paleogeographic and tectonic consequences. – *Int. Journ. Earth Sci.*, **88**, 201-218.
- GASQUET D. (1979). – Etude pétrologique, géochimique et structurale des terrains cristallins de Belledonne et du Grand Chatelard traversés par les galeries EDF Arc-Isère, Alpes françaises. – Thèse 3^{ème} cycle, Université de Grenoble, 231 p.
- GUETTY S.R. & DE PAOLO D.J. (1995). – Quaternary geochronology using the U-Th-Pb method. – *Geochim. Cosmochim. Acta*, **59**, 3267-3272.
- GIDON M. & PAIRIS J.-L. (1992). – Relations entre le charriage de la nappe de Digne et la structure de son autochtone dans la vallée du Bès (Alpes de Haute-Provence, France). – *Eclogae geol. Helv.*, **85**, 327-359.
- GOURLAY P. (1984). – La déformation alpine des massifs cristallins externes du Mont Blanc, Aiguilles Rouges, Belledonne) et celle de leur couverture mésozoïque (Alpes occidentales). – Thèse 3^{ème} cycle, Université Paris 6, 130p.
- HARRISON T.M., MCKEEGAN K.D. & LEFORT P. (1995). – Detection of inherited monazite in the Manaslu leucogranite by $^{208}\text{Pb}/^{232}\text{Th}$ ion microprobe dating; crystallization age and tectonic implications. – *Earth Planet. Sci. Lett.*, **133**, 271-282.
- HIPPOLYTE J.-C., CLAUZON G., BELLIER O., LAROQUE C. & MOLLIEUX S. (2008). – Reconstitution du réseau hydrographique et quantification de la déformation récente dans les Alpes du Sud (nappe de Digne, arc de Nice). – Séance spécialisée Soc. géol. Fr. *Géodynamique et paléogéographie de l'aire méditerranéenne au Mio-Pliocène*, Lyon, 5-6 Mai 2008. – Résumés, p.44.
- HUBBARD M. & MANCKTELOW N. (1992). – Lateral displacement during Neogene convergence in the western and central Alps. – *Geology*, **20**, 943-946.

- HUESTIS S.P. & ACTON G.D. (1997). – On the construction of geomagnetic timescales from non-prejudicial treatment of magnetic anomaly data from multiple ridges. – *Geophys. J. Int.*, **129**, 176-182.
- JACKSON S.E., PEARSON N.J., GRIFFIN W.L. & BELOUSOVA E.A. (2004). – The application of laser ablation-inductively coupled plasma-mass spectrometry to in situ U-Pb zircon geochronology. – *Chem. Geol.*, **211**, 47-69.
- KIRSCHNER L., COSCA M.A., MASSON H. & HUNZIKER J.C. (1996). – Staircase $^{40}\text{Ar}/^{39}\text{Ar}$ spectra of fine-grained white mica: timing and duration of deformation and empirical constraints on argon diffusion. – *Geology*, **24**, 747-750.
- KRIJGSMAN W., BLANC-VALLERON M.-M., FLECKER R., HILGEN F.J., KOUWENHOVEN T.J., MERLE D., ORSZAG-SPERBER F. & ROUCHY J.-M. (2002). – The onset of the Messinian salinity crisis in the eastern Mediterranean (Pissouri basin, Cyprus). – *Earth Planet. Sci. Lett.*, **194**, 299-310.
- LEDRU P., COURRIOUX G., DALLAIN C., LARDEAUX J.-M., MONTEL J.-M., VANDERHAEGHE O. & VITEL G. (2001). – The Velay dome (French Massif Central): melt generation and granite emplacement during orogenic evolution. – *Tectonophysics*, **342**, 207-237.
- LEHMANN J. (2004). – Chronologie relative des déformations alpines en bordure orientale du massif de la Lauzière (Alpes occidentales). Etude en lame mince. – Mémoire Maîtrise, Université Joseph Fourier, Grenoble.
- LELOUP P.H., ARNAUD N., SOBEL E.R. & LACASSIN R. (2005). – Alpine thermal and structural evolution of the highest external crystalline massif: The Mont Blanc. – *Tectonics*, **24**, TC4002, doi: 10.1029/2004TC001676, 26p.
- LELOUP P.H., ARNAUD N., SOBEL E.R. & LACASSIN R. (2007). – Reply to comment by Y. Rolland *et al.* on “Alpine thermal and structural evolution of the highest external crystalline massif: The Mont Blanc”. – *Tectonics*, **26**, TC2016, doi: 10.1029/2006TC002022
- LEUTWEIN F., POTY B., SONET J. & ZIMERMANN J.-L. (1970). – Age des cavités à cristaux du granite du Mont-Blanc. – *C.R. Acad. Sci.*, Paris, **271**, 156-158.
- MARQUER D. (1987). – Transfert de matière et déformation progressive des granitoïdes. Exemple des massifs de l’Aar et du Gothard (Alpes centrales suisses). – PhD Thesis, Mémoires et Documents du Centre Armoricain d’Etudes Structurales des Socles, Université de Rennes, 10, 250 pp.
- MARSHALL D., MEISSER N. & TAYLOR R.P. (1998). – Fluid inclusion, stable isotope and Ar-Ar evidence for the age and origin of gold-bearing quartz veins at Mont Chemin, Switzerland. – *Mineral. Petrol.*, **62**, 147-165.
- NEGGA H.S. (1984). – Comportement de l’uranium lors des métamorphismes tardi-hercynien et alpin dans les massifs des Aiguilles Rouges et de Belledonne (Vallorcine, Lauzière, Alpes occidentales). – PhD, Université de Nancy, 419 p.
- NZIENGUI J.J. (1993). – Excès d’argon radiogénique dans les quartz des fissures tectoniques : implications pour la datation des séries métamorphiques. L’exemple de la coupe de la Romanche, Alpes occidentales françaises. – Thèse 3^{ème} cycle, Univ. Grenoble, 209 p.
- PAQUETTE J.-L. & PIN C. (2001). – A new miniaturized extraction chromatography method for precise U-Pb geochronology. – *Chem. Geol.*, **176**, 311-319.
- PAQUETTE J.-L. & TIEPOLO M. (2007). – High resolution (5 microns) U-Th-Pb isotope dating of monazite with excimer laser ablation (ELA)-ICPMS. – *Chem. Geol.*, **240**, 222-237.
- PETTKE T., DIAMOND L.W. & VILLA I. (1999). – Mesothermal gold veins and metamorphic devolatilization in the northwestern Alps: the temporal link. – *Geology*, **27**, 641-644.
- PONCERRY E. (1981). – Contribution à l’étude des granitoïdes de Vallorcine, Beaufort, Lauzière, de leur encaissant et des minéralisations uranifères associées, Alpes françaises. – Thèse 3^{ème} cycle, Université de Grenoble, 319 p.
- POTY B. (1969). – La croissance des cristaux de quartz dans les filons sur l’exemple du filon de La Gardette (Bourg d’Oisans) et des filons du massif du Mont-Blanc. – PhD thesis, Université de Nancy, 161 p.
- POTY B., STADLER H.A. & WEISBROD A.M. (1974). – Fluid inclusions studies in quartz from fissures of the western and Central Alps. – *Schweiz. Mineral. Petrogr. Mitt.*, **54**, 717-752.
- RATZOV G. (2004). – Chronologie relative des déformations alpines en bordure orientale du massif de la Lauzière (Alpes occidentales). Etude de terrain. – Mémoire Maîtrise, Université Joseph Fourier, Grenoble.
- ROLLAND Y., COX S. F., BOULLIER A.-M., PENNACHIONI G. & MANCKTELOW N. (2003). – Rare earth and trace element mobility in mid-crustal shear zones: insights from the Mont Blanc Massif (western Alps). – *Earth Planet. Sci. Lett.*, **214**, 203-219.
- ROLLAND Y., CORSINI M., ROSSI M., COX S.F., PENNACHIONI G., MANCKTELOW N., BOULLIER A.-M. & FORNARI M. (2007). – Comment on the dating of Alpine deformation by Ar-Ar on syn-kinematic mica in mid-crustal shear zones of the Mont Blanc Massif (paper by Leleoup *et al.*). – *Tectonics*, **26**, TC2015, doi 10: 1029/2006TC001956.
- ROLLAND Y., ROSSI M., COX S.F., CORSINI M., MANCKTELOW N., PENNACHIONI G., FORNARI M. & BOULLIER A.-M. (2008). – $^{40}\text{Ar}/^{39}\text{Ar}$ dating of synkinematic white mica: insights from fluid-rock reaction in low-grade shear zones (Mont Blanc Massif) and constraints on timing of deformation in the NW external Alps. – *Geol. Soc., London, Sp. Publ.*, **299**, 293-315
- ROSSI M. (2005). – Déformation, transferts de matière et de fluide dans la croûte continentale: application aux massifs cristallins externes des Alpes. – Ph.D. thesis, Joseph Fourier University, Grenoble, 388p.
- ROSSI M., ROLLAND Y., VIDAL O. & COX S.F. (2005). – Geochemical variations and element transfer during shear zone development and related episyenites at middle crust depths: insights from the study of the Mont-Blanc Granite (French-Italian Alps). – *Geol. Soc. London Sp. Publ.*, **245**, 373-396.
- SCAILLET S. (1996). – Excess ^{40}Ar transport scale and mechanism in high-pressure phengites: A case study from an eclogitized metabasite of the Dora-Maira nappe, western Alps. – *Geochim. Cosmochim. Acta*, **60**, 1075-1090.
- SCAILLET S. (2000). – Numerical error analysis in $^{40}\text{Ar}/^{39}\text{Ar}$ dating. – *Chem. Geol.*, **162**, 269-298.
- SCHÄRER U. (1984). – The effect of initial ^{230}Th disequilibrium on young U-Pb ages: the Makalu case, Himalaya. – *Earth Planet. Sci. Lett.*, **67**, 191-204.
- SCHLUNEGGER F., RIEKE-ZAPP D. & RAMSEYER K. (2007). – Possible environmental effects on the evolution of the Alps-Molasse Basin system. – *Swiss J. Geosci.*, **100**, 383-405.
- SEYDOUX-GUILLAUME A.M., PAQUETTE J.-L., WIEDENBECK M., MONTEL J.M. & HEINRICH W. (2002). – Experimental resetting of the U-Th-Pb system in monazite. – *Chem. Geol.*, **191**, 165-181.
- SEYDOUX-GUILLAUME A.M., WIRTH R., DEUTSCH A. & SCHÄRER U. (2004). – Microstructure of 24-1928 Ma concordant monazites; implications for geochronology and nuclear waste deposits. – *Geochim. Cosmochim. Acta*, **68**, 2517-2527.
- STACEY J.S. & KRAMERS J.D. (1975). – Approximation of terrestrial lead isotope evolution by a two-stage model. – *Earth Planet. Sci. Lett.*, **26**, 207-221.
- STERN R. A. & SANDBORN N. (1998). – Monazite U-Pb and Th-Pb geochronology by high-resolution secondary ion mass spectrometry. Radiogenic age and isotopic studies. – Report 11 Geol. Surv. Can Curr. Res, 1-18.
- TIEPOLO M., BOTTAZZI P., PALENZONA M. & VANNUCCI R. (2003). – A laser probe coupled with ICP-double-focusing sector-field mass spectrometer for in situ analysis of geological samples and U-Pb dating of zircon. – *Can. Mineral.*, **41**, 259-272.
- THIRLWALL M.F. (2002). – Multicollector ICP-MS analysis of Pb isotopes using a ^{207}Pb - ^{204}Pb double spike demonstrates up to 400 ppm/amu systematic errors in TI-normalization. – *Chem. Geol.*, **184**, 255-279
- VAN ACHTERBERGH E., RYAN C.G., JACKSON S.E. & GRIGGIN W. (2001). – Data reduction software for LA-ICP-MS. In: P. SYLVESTER, Ed., Laser ablation ICPMS in the Earth Science. – *Mineralogical Association of Canada*, **29**, 239-343.
- WILLETT S., SCHLUNEGGER F. & PICOTTI V. (2006). – Messinian erosion of the Alps and its implications for Neogene climate change. – *Geology*, **34**, 613-616.
- VON RAUMER J. (1984). – The External Massifs, relics of Variscan basement in the Alps. – *Int. J. Earth Sci.*, **73**, 1-31.